Ultraviolet-infrared dielectric functions and electronic band structures of monoclinic VO_2 nanocrystalline film: Temperature-dependent spectral transmittance

W. W. Li (李文武),[1] J. J. Zhu (诸佳俊),[1] X. F. Xu (徐晓峰),[2] K. Jiang (姜凯),[1] Z. G. Hu (胡志高),[1,a)] M. Zhu (朱敏),[3] and J. H. Chu (褚君浩)[1]
[1]*Key Laboratory of Polar Materials and Devices, Ministry of Education, Department of Electronic Engineering, East China Normal University, Shanghai 200241, China*
[2]*Department of Applied Physics, Donghua University, Shanghai 201620, China*
[3]*Department of Physics, Shanghai Jiao Tong University, Shanghai 200240, China*

(Received 10 March 2011; accepted 16 May 2011; published online 1 July 2011)

Nanocrystalline vanadium dioxide (VO_2) film on *c*-plane sapphire substrate has been prepared by direct-current magnetron sputter deposition. The electronic band structures of the VO_2 film with monoclinic phase have been investigated by ultraviolet-infrared transmittance spectra in the temperature range of 5.3–300 K. It was found that the transmittance decreases while the dielectric functions slightly increase with the temperature. The optical bandgap decreases from 0.839 ± 0.003 to 0.788 ± 0.003 eV with increasing the temperature due to the variations of lattice constant and V_d-O_p hybridization. Moreover, three higher-order interband electronic transitions can be uniquely distinguished and the temperature effects on the higher-order transition energy become much weaker. © *2011 American Institute of Physics*. [doi:10.1063/1.3601357]

I. INTRODUCTION

For several decades, transition metal oxides have received much attention in view of their fascinating properties and wide applications. In particular, electronic structures and optical properties in transition metal oxides are of fundamental importance and applied interest. One of the most widely studied materials is vanadium dioxide (VO_2), which has attracted considerable attention with regard to its potential applications in smart windows, optical storage devices, infrared detectors, etc.[1–4] At temperatures above 340 K, VO_2 is metallic with the tetragonal structure, where overlap between the Fermi level and the V 3*d* band eliminates the bandgap. At temperatures below 340 K, however, it forms the monoclinic (*M*) structure with space group $P2_1/c$ and becomes an insulator. A striking feature of the *M* phase is that the dimerization of V atoms with the zigzaglike displacements.[5] The unit cell doubles in size and neighboring V^{4+} form a twisted pair with a lowered symmetry. The splitting of V^{4+} 3*d* states leads to a gap between empty e_g^{π} band and filled a_{1g} band, with the bandgap energy $E_g \approx 0.7$ eV.[6,7] Moreover, the high dielectric constants and visible transmittance make *M* phase VO_2 a promising material for low temperature optoelectronic device and glass surface design. Therefore, it is desirable to thoroughly investigate the electronic structures and optical properties of *M* structure VO_2 films.

The electronic and optical response behaviors of VO_2 films are not only dependent on thickness and doping elements but also sensitive to external perturbations such as temperature, pressure, and electric fields. Early research indicated that the optical bandgap (OBG) of VO_2 film decreases from about 0.77 to 0.57 eV when the thickness is reduced from 31 to 6 nm.[8] Furthermore, the optical constants of *M* phase VO_2 have been determined at the photon energy from 0.25 to 5 eV.[9] The singularities in the imaginary part of dielectric functions have been assigned to the specific interband transitions. However, there are few systematical reports concerning the dielectric functions, electronic transition, and OBG at low temperatures, especially for the temperature dependence of the higher-order interband transitions. As an element, the VO_2-based field effect transistor can be used to realize fully planar integrated infrared focal plane arrays.[10] In order to make sure the device works well at low temperature, understanding and describing the optical constants, electronic excitations, and absorption coefficient of VO_2 films at low temperature are the pre-requisite. Temperature dependence of the OBG energy from the interband transitions can provide the important information about the electron-phonon interactions and collective excitations. In addition, it is important for the elucidation of the actual electronic states and understanding the role of the electronic contribution to the optical properties for VO_2 material. It should be emphasized that the transmittance technique is widely acceptable and applied in the case of transparent substrates, which can directly present the transmission and/or absorption of material system studied. It is easy and useful to derive the dielectric functions of VO_2 film by subtracting the contributions from transparent sapphire substrates.[11]

In this paper, the dielectric functions, OBG, and electronic transitions of VO_2 film on *c*-plane sapphire substrate have been investigated by spectral transmittance technique. A dielectric function theoretical model is presented to reproduce the experimental transmittance spectra well. The temperature influences on the electronic band structures have been discussed in detail.

a)Author to whom correspondence should be addressed. Electronic mail: zghu@ee.ecnu.edu.cn.

II. EXPERIMENT

Nanocrystalline VO_2 film was prepared on *c*-plane sapphire substrate by direct-current magnetron sputter deposition. The vacuum chamber was evacuated down to 5×10^{-5} Pa and then filled into the argon gas. Under the conditions of 1 Pa and 45 W, metallic vanadium film was deposited on the substrate at room temperature (RT). The diameter of target was 60 mm. The distance between target and substrate was fixed at 120 mm. The substrate was rotated at 13 rpm to ensure uniformity of film deposition. In order to eliminate contamination on the target surface, pre-sputtering of the vanadium metal target was performed before depositing the metallic vanadium film. After deposition, the vanadium metal film was taken out from the chamber, and then put it on the furnace for further oxidation in air atmosphere. The temperature was fixed at 743 K for 2 h to ensure the temperature stability. A detailed preparation of the film has been described elsewhere.[12]

The crystalline structure of the VO_2 film was analyzed by x-ray diffraction (XRD) using Cu $K\alpha$ radiation (D/MAX-2550V, Rigaku Co.). The electrical properties while heating and cooling across the metal-insulator transition were measured by four-point probe method. The normal-incident transmittance spectra were recorded at 5.3–300 K using a double beam ultraviolet-infrared spectrophotometer (PerkinElmer Lambda 950) at the photon energy from 0.5 to 6.5 eV (190–2650 nm) with a spectral resolution of 2 nm. The VO_2 film and sapphire substrate were mounted into an optical cryostat (Janis SHI-4-1) for low temperature experiments, respectively. Note that the temperature interval is about 10 and 25 K for the two different regions of 5.3–125 and 125–300 K, respectively. To eliminate the effects from the windows of cryostat, the transmittance spectrum of the quartz windows was also recorded.

III. RESULTS AND DISCUSSIONS

The peak at about 41.81° is originated from the (006) diffraction peak of *c*-plane sapphire substrate, as shown in Fig. 1(a). As compared to the standard reference data (JCPDS No. 76-0673 and No. 71-0290), the other three peaks can be attributed to the (001), (021), and (002) diffraction peaks of VO_2 material. It confirms that the VO_2 film is of the monoclinic phase. Moreover, it should be noticed that there is some presence of vanadium pentoxide (V_2O_5) due to some crystalline imperfections and inhomogeneities of the film, which remain strong even on a microscopic level. Therefore, it is also possible that the peak appearing at about 20.58° is originated from the (001) plane of V_2O_5 phase. Note further that the crystalline quality of the prepared VO_2 film in this work is different from other samples, which can be ascribed to different intrinsic defects, stoichiometry, film inhomogeneities, and growth technique. As compared to other reports,[13,14] the crystalline orientation varied from sample to sample due to different crystalline quality. In order to further study the film quality and stoichiometry, the temperature dependence of sheet resistances for both heating and cooling processes were measured and shown in the inset of Fig. 1(a). The sheet resistances show a hysteresis behavior

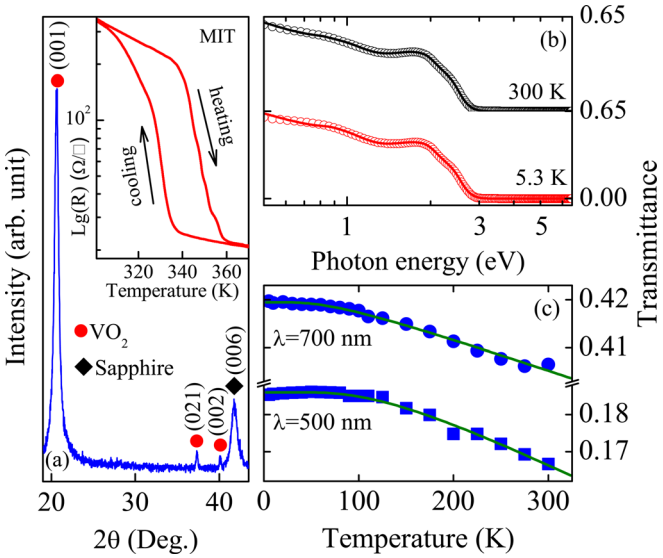

FIG. 1. (Color online) (a) The x-ray diffraction pattern of the VO_2 film on sapphire substrate. The label "◆" denotes the (006) diffraction peak at about 41.81° from *c*-plane sapphire substrate. The inset shows the temperature dependence of the sheet resistances when the heating and cooling is across the metal-insulator transition. (b) The experimental (dotted curves) and fitting (solid curves) transmittance spectra at temperatures of 300 and 5.3 K, respectively. The horizontal coordinate is the logarithmic unit to enlarge the transparent region. (c) Temperature dependence of the transmittance at wavelengths of 700 and 500 nm, respectively (dotted curve). The solid lines are the fitting results to guide the eyes.

and the typical metal-insulator transition can be observed. It indicates that the temperature for the onset of reverse transition is clearly delayed. Moreover, the large magnitude change in the sheet resistances suggest that the film quality and stoichiometry can be reasonably acceptable, which is in agreement with with the XRD results.

The inverse synthesis method is based on a phenomenological model fitted to the experimental results. The reliability of the inverse synthesis method mainly depends on the validity of the optical model and the fitting statistics. For the VO_2 film, the dielectric functions can be derived by fitting the transmittance spectra with double Tauc–Lorentz (DTL) oscillators:[15–17]

$$\varepsilon_1(E) = \varepsilon_\infty + \frac{2}{\pi} P \int_0^\infty \frac{\xi \varepsilon_2(E)}{\xi^2 - E^2} d\xi;$$
$$\varepsilon_2(E) = \sum_{i=1}^{2} \frac{A_i E_{pi} \Gamma_i (E - E_{ti})^2}{(E^2 - E_{pi}^2)^2 + \Gamma_i^2 E^2} \frac{1}{E}, \quad (1)$$

where ε_∞ is the high-frequency dielectric constant, P is the Cauchy principal part of the integral, E is the incident photon energy, A_i, E_{pi}, Γ_i, and E_{ti} is the amplitude, peak position energy, broadening term, and Tauc gap energy of the ith oscillator, respectively. It should be emphasized that the DTL model, which abides by the Kramers–Krönig transformation in the entirely measured photon energy region, is successfully applied in many semiconductor and dielectric materials.[16] A least-squares-fitting procedure employing the modified Levenberg–Marquardt algorithm is used in the fitting. The fitting is a process of minimizing the deviation parameter with the optimized values of the fitting parameters. As an example,

the experimental and fitting transmittance spectra of the VO_2 film at 300 and 5.3 K are shown in Fig. 1(b). A good agreement is obtained between the experimental and calculated spectra, especially at short wavelength region. The transmittance spectra are similar to those prepared on quartz substrates.[18] Furthermore, the transmittance spectra shift toward the lower energy side with the temperature, suggesting that the bandgap of the film has a negative temperature coefficient. Figure 1(c) presents the temperature dependent transmittance at the wavelengths of 700 and 500 nm, respectively. Note that the transmittance at 700 nm (42%) is higher than that prepared by solution-phase synthesis (26%) with the comparable thickness at RT.[3] With decreasing the temperature, the transmittance of the film evidently increases and finally keeps as a constant. This is because the bandgap of the film, which is broadening at low temperature, is different under the distinct temperature regions. It can weaken the electronic transitions and result in less interband absorptions.

For a comparison, the DTL parameter values of the VO_2 film at 300, 200, and 5.3 K are listed in Table I. The thickness of the VO_2 film was estimated to 135 ± 1 nm by fitting the transmittance spectra recorded at RT. As can be seen in Table I, the A_1 value decreases while the A_2 value increases with the temperature. It indicates that the temperature influences on the strength of the different optical transition are disparate. Moreover. the ε_∞ and Γ_i values increase with the temperature. The evaluated dielectric functions of the VO_2 film are shown in Fig. 2, which agree well with the theoretical and experimental results.[19,20] Both the real part ε_1 and imaginary part ε_2 values increase with the temperature. The ε_1 and ε_2 redshift at the lower photon energy while the dielectric functions blueshift with further increasing the photon energy. This is because the electronic orbital hybridization, band splitting, and atom interaction strongly affected by the temperature, which result in the modification of electronic band structures. In addition, the phenomena are also related to the electron-phonon interaction and the lattice thermal expansion with the temperature. The electron-electron interaction, which is necessary to produce the bandgap in the insulating phase, is important to fully understand the electronic structures and charge transport in the VO_2 film.[21] The number of optical transition is related to the physical properties of the VO_2 films. Based on the previous theoretical calculations and experimental observations, four transitions at the photon energy from ultraviolet to near-infrared and the assignments have been widely accepted.[20,22] For the present VO_2 film, four features can be also clearly identified

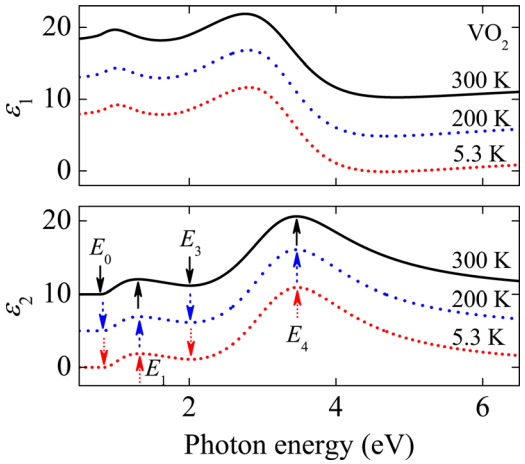

FIG. 2. (Color online) Real part and imaginary part of the dielectric function in the VO_2 film at temperatures of 300, 200, and 5.3 K, respectively. Note that both ε_1 and ε_2 values are vertically shifted by adding 5. The arrows indicate the energy positions of the electronic transitions.

from the ε_2 curves and are labeled with E_0, E_1, E_3, and E_4, respectively. The characteristics correspond to the different interband electronic transitions between filled and empty bands in the VO_2 film. The interband optical transitions are governed by the electric dipole transition matrix elements and peaks in the joint density of (filled and empty) states.[22] From Table I, the broadening parameter values are relatively large, as compared to the transition energy. Therefore, the transition band from the dielectric functions could be ascribed to the large Γ values.

In the M phase VO_2 film, the crystal field splits the degenerate d orbitals into t_{2g} bands and e_g^σ bands. The t_{2g} bands, which are lower in energy and contain the single d electron, are further split into a lower a_{1g} band and upper e_g^π bands. The V^{4+}-V^{4+} pairing along the c axis splits a_{1g} band into lower and upper a_{1g} bands. Moreover, the twisting of V^{4+}-V^{4+} pairs increases V_d-O_p hybridization and lifts e_g^π band above Fermi energy (E_F) so that only the lower a_{1g} band is filled.[5,6,22] The E_0 threshold, which corresponds to an indirect bandgap energy between Z and C points in the Brillouin zone (BZ), can be assigned to the indirect transition from the top of filled a_{1g} band (E_v) to the bottom of empty e_g^π band (E_c) when the photon energy falls on materials. The power law behavior of Tauc is $(\alpha E)^{1/2} \propto (E - E_g)$ for allowed indirect transition, where E_g is the OBG energy and $\alpha = 4\pi k/\lambda$ is the absorption coefficient. So the straight line between $(\alpha E)^{1/2}$ and E will provide the E_g value, which is extrapolated

TABLE I. The double Tauc–Lorentz parameter values of the VO_2 film are determined from the simulation of the transmittance spectra at 300, 200, and 5.3 K, respectively.

Temperature (K)	ε_∞	Oscillator	A (eV)	E_p (eV)	Γ (eV)	E_t (eV)
300	3.10 ± 0.11	TL1	19.5 ± 1.3	1.02 ± 0.02	0.89 ± 0.02	0.79 ± 0.01
		TL2	99.2 ± 3.4	3.29 ± 0.01	1.81 ± 0.06	1.89 ± 0.01
200	2.89 ± 0.13	TL1	21.8 ± 1.5	1.00 ± 0.02	0.85 ± 0.02	0.82 ± 0.01
		TL2	94.2 ± 3.6	3.32 ± 0.02	1.69 ± 0.06	1.89 ± 0.01
5.3	2.88 ± 0.16	TL1	22.9 ± 2.2	0.99 ± 0.03	0.80 ± 0.03	0.84 ± 0.01
		TL2	92.7 ± 4.5	3.33 ± 0.02	1.69 ± 0.08	1.89 ± 0.01

by the linear portion of the plot to $(\alpha E)^{1/2}=0$. As can be seen from Fig. 3(a), the OBG value decreases from 0.839 ± 0.003 to 0.788 ± 0.003 eV, corresponding to increasing the temperature from 5.3 to 300 K, which indicates that the total redshift value of the bandgap is about 50 meV. It supports the conclusion that the temperature-induced increase in the spectral transmittance are ascribed to the bandgap broadening. The observed decrease in the E_g with the temperature can be described using the Bose–Einstein model, in which the carrier-phonon coupling is taken into account, and can be given as

$$E_g(T) = E_g(0) - \frac{2a_B}{\exp(\Theta_B/T) - 1}, \quad (2)$$

where $E_g(0)$ represents the OBG energy toward 0 K, a_B is the strength of the electron-phonon interaction, $\Theta_B \equiv \hbar\nu/k_B$ is the characteristic temperature representing the effective phonon energy on the temperature scale, and T is the experimental temperature. The fitting result indicates that the $E_g(0)$ value is about 0.840 eV. The parameters a_B and Θ_B are 118 meV and 523 K, respectively. These values are larger than that from other insulator materials such as $BiFeO_3$ film (21 meV and 238 K).[16] With decreasing temperature, the lattice constant of the VO_2 film was changed due to the dilatation of lattice and the shortening of interatomic distances. The e_g^π bands are shifted to the higher energy while the bonding a_{1g} peak was contracted. The E_c upward and the E_ν downward for the VO_2 film induce the broadening of the bandgap. In addition, the V-V pair twisting and V_d-O_p hybridization are expected to move the V^{4+} 3d valence band. The changes in charge localization are believed to shift the 3d conduction band. It can also result in the OBG redshift.[6]

The E_1 feature can be assigned to the transition from the lower V 3d filled a_{1g} band to the crystal field split 3d empty e_g^π bands across the optical gap at other points in the BZ. It was reported that the filled a_{1g} orbitals cannot transfer to the nearest-neighbor V atoms along the c axis. Furthermore, the a_{1g} orbitals between the second-nearest-neighbor V atoms are orthogonal. Therefore, the E_1 transition should occur between the second-nearest-neighbor V atoms.[23] With increasing temperature, the E_1 transition energy shifts from 1.325 ± 0.003 to 1.304 ± 0.003 eV, as shown in Fig. 3(b). Compared to the previous reports,[19,20,22] the E_3 feature located at about 2.01 eV is not evident due to different growth method and crystalline quality. The value is larger than that observed by Gavini *et al.* while less than that found by Continenza *et al.*[19,20] The E_3 critical point can be interpreted to the transition between the lower V 3d filled a_{1g} band and the upper empty a_{1g} band. As can be seen from Fig. 3(c), the E_3 transition energy redshifts from 2.021 ± 0.003 to 2.006 ± 0.003 eV with the temperature. In the insulating phase, the V 3d band is broadened as the temperature is increased, which is responsible for the redshift of E_1 and E_3 transition energy.[21] Note that the variation tendency of E_1 and E_3 with the temperature can be also expressed by the Bose–Einstein model. However, the highest order transition E_4 slowly decreases with the temperature and does not follow the Bose–Einstein relationship. The transition can be assigned to the excitation from the filled O_{2p} bands to the empty e_g^π bands.[20,22] The e_g^π bands are shifted to the lower energy, which lead to the transition energy shows a decreasing trend in general with the temperature. However, the strongly V_d-O_p hybridization and V-V interaction obviously changed at different temperature, which may not follow the Bose–Einstein formula. It will drive the O 2p bands correspondingly shifted with the temperature. Moreover, the higher electronic transition would result in higher electronic density of states in O 2p states. Therefore, the above mechanisms can contribute to the E_4 transition and induce the abnormal variation.[6]

To understand the above analysis, the schematic diagram of electronic band structures and transitions are summarized in Fig. 4(a). It should be emphasized that there are both acceptor and donor states within the bandgap of VO_2 insulating phase. The integrated density is typical between 10^{19} and 10^{20} cm^{-3}. These states are likely to arise from the crystalline imperfections such as oxygen vacancies, interstitial V ions, dislocations, domain boundaries, and cracks.[24] However, the optical transition into and out of the acceptor

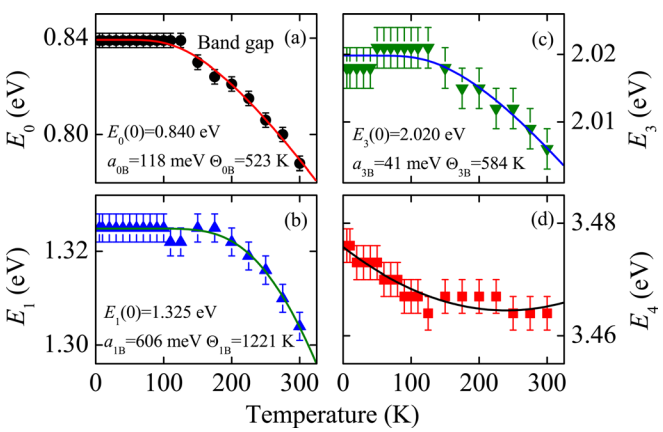

FIG. 3. (Color online) The four electronic transition energies as a function of temperature (a) E_0, (b) E_1, (c) E_3, and (d) E_4. The variations of E_0, E_1, and E_3 transitions with the temperature were fitted by the Bose–Einstein model.

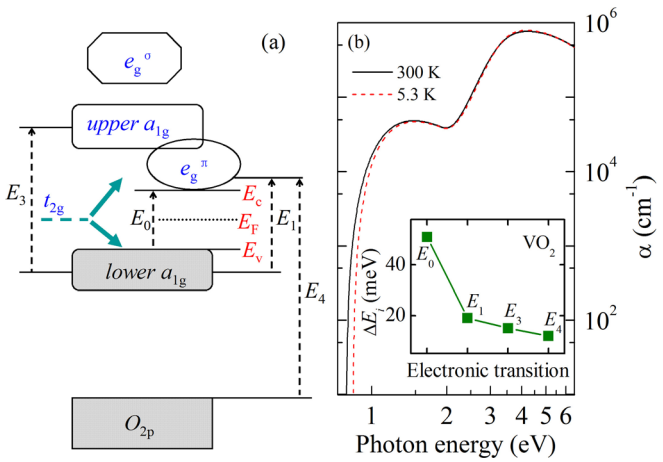

FIG. 4. (Color online) (a) The schematic diagram of electronic band structures and transitions in the VO_2 film. (b) The absorption coefficient α at temperatures of 300 and 5.3 K, respectively. The inset shows that the total shift of transition energy corresponds to each electronic transition.

and donor levels cannot be detected within the instrumental sensitivity. On the other hand, the fact that the density is well below the density of V ions and the energy distribution is structureless could be another possible cause. Therefore, it is difficult to determine the actual acceptor and donor levels, so that the levels are not plotted in Fig. 4(a). Nevertheless, the temperature-dependent acceptor and donor states can mask the optical absorption threshold at the bandgap energy. It will further influence the inter-band transition at different temperature in the VO_2 film.[24]

The a_B values can reflect the strength of the coupling between the phonons and the electronic at different band edges. In particular, the interaction with longitudinal optical (LO) phonons will increase with the ionicity. Since the strength of the a_B in the E_1 transition is stronger than that in the E_0 and E_3 transitions, the LO phonon replicas of the exciton transition are expected to be steadily enhanced in E_1 than in E_0 and E_3. Furthermore, the Θ_B values increase with the order of electronic transitions. The larger effective phonon energy indicates a larger acoustic phonon contribution to the states of conduction band. In addition, the total shift of transition energy is 51, 21, 15, and 12 meV, respectively, with the order of electronic transitions, as presented in the inset of Fig. 4(b). It suggests that the temperature effects on the higher-order transition energy become much weaker. Note that the thermal strain and substrate-induced strain cannot be considered by comparing the lattice constant mismatch and film thickness in the present work. On the other hand, the contributions from the polycrystalline structure of the VO_2 films can be much larger than those from the strains, which should be neglected.[25]

The absorption coefficient is one of the important parameters for the VO_2 film in the infrared detectors and arrays. Figure 4(b) displays the absorption coefficient of the VO_2 film at temperatures of 300 and 5.3 K, respectively. Note that the critical points related to the interband electronic transitions can be discerned again from the spectra. The α value increases with the temperature at the lower photon energy while keeps as a constant with further increasing the photon energy. The photon energy corresponding to $\alpha = 10^4$ cm^{-1} decreases from 0.983 to 0.950 eV with increasing the temperature, which agrees with the observed variation trend from the OBG and suggests that the total redshift value is about 33 meV. The photon energy value at RT is larger than the OBG value and that from VO_2 single crystal.[9] In addition, the α value at RT rapidly increases from 10^3 cm^{-1} at 0.836 eV to 10^5 cm^{-1} at 0.947 eV. The large values of absorption coefficient indicate that the V 3*d* bands are strongly hybridized with the O 2*p* bands.

IV. CONCLUSION

In conclusion, the dielectric functions, optical bandgap, and electronic transitions of monoclinic VO_2 nanocrystalline film have been investigated using ultraviolet-infrared transmittance spectra in the temperature range of 5.3–300 K. It was found that the dielectric functions strongly depend on the temperature. Four electronic transitions can be assigned and the energies decrease with increasing the temperature. Furthermore, the bandgap energy decreases with increasing the temperature.

ACKNOWLEDGMENTS

This work was financially supported by Natural Science Foundation of China (Grant Nos. 60906046 and 11074076), Major State Basic Research Development Program of China (Grant Nos. 2007CB924901 and 2011CB922200), Program of New Century Excellent Talents, Ministry of Education (Grant No. NCET-08-0192) and PCSIRT, Projects of Science and Technology Commission of Shanghai Municipality (Grant Nos. 10DJ1400201, 10SG28, 10ZR1409800, and 09ZZ42), and the Program for Professor of Special Appointment (Eastern Scholar) at Shanghai Institutions of Higher Learning.

[1]M. M. Qazilbash, M. Brehm, B. G. Chae, P. C. Ho, G. O. Andreev, B. J. Kim, S. J. Yun, A. V. Balatsky, M. B. Maple, F. Keilmann, H. T. Kim, and D. N. Basov, Science **318**, 1750 (2007).
[2]C. Ko and R. Ramanathan, Appl. Phys. Lett. **93**, 252101 (2008).
[3]Z. T. Zhang, Y. F. Gao, Z. Chen, J. Du, C. X. Cao, L. T. Kang, and H. J. Luo, Langmuir **26**, 10738 (2010).
[4]R. Sakuma, T. Miyake, and F. Aryasetiawan, Phys. Rev. B **78**, 075106 (2008).
[5]J. Goodenough, J. Solid State Chem. **3**, 490 (1971).
[6]C. H. Chen and Z. Y. Fan, Appl. Phys. Lett. **95**, 262106 (2009).
[7]S. Biermann, A. Poteryaev, A. I. Lichtenstein, and A. Georges, Phys. Rev. Lett. **94**, 026404 (2005).
[8]H. K. Kim, H. You, R. P. Chiarello, H. L. M. Chang, T. J. Zhang, and D. J. Lam, Phys. Rev. B **47**, 12900 (1993).
[9]H. W. Verleur, A. S. Barker, Jr., and C. N. Berglund, Phys. Rev. **172**, 788 (1968).
[10]C. H. Chen and Z. P. Zhou, Appl. Phys. Lett. **91**, 011107 (2007).
[11]W. W. Li, J. J. Zhu, J. D. Wu, J. Sun, M. Zhu, Z. G. Hu, and J. H. Chu, ACS Appl. Mater. Interfaces **2**, 2325 (2010).
[12]X. F. Xu, A. Y. Yin, X. L. Du, J. Q. Wang, J. D. Liu, X. F. He, X. X. Liu, and Y. L. Huan, Appl. Surf. Sci. **256**, 2750 (2010).
[13]S. Lysenko, V. Vikhnin, F. Fernandez, A. Rua, and H. Liu, Phys. Rev. B **75**, 075109 (2007).
[14]T. -H. Yang, R. Aggarwal, A. Gupta, H. H. Zhou, R. J. Narayan, and J. Narayan, J. Appl. Phys. **107**, 053514 (2010).
[15]G. E. Jellison, Jr. and F. A. Modine, Appl. Phys. Lett. **69**, 371 (1996); G. E. Jellison, Jr. and F. A. Modine, Appl. Phys. Lett. **69**, 2137 (1996).
[16]W. W. Li, J. J. Zhu, J. D. Wu, J. Gan, Z. G. Hu, M. Zhu, and J. H. Chu, Appl. Phys. Lett. **97**, 121102 (2010).
[17]Z. G. Hu, J. H. Ma, Z. M. Huang, Y. N. Wu, G. S. Wang, and J. H. Chu, Appl. Phys. Lett. **83**, 3686 (2003).
[18]L. T. Kang, Y. F. Gao, Z. T. Zhang, J. Du, Z. Chen, and H. J. Luo, J. Phys. Chem. C **114**, 1901 (2010).
[19]A. Continenza, S. Massidda, and M. Posternak, Phys. Rev. B **60**, 15699 (1999).
[20]A. Gavini and C. C. Y. Kwan, Phys. Rev. B **5**, 3138 (1972).
[21]K. Okazaki, H. Wadati, A. Fujimori, M. Onoda, Y. Muraoka, and Z. Hiroi, Phys. Rev. B **69**, 165104 (2004).
[22]M. M. Qazilbash, A. A. Schafgans, K. S. Burch, S. J. Yun, B. G. Chae, B. J. Kim, H. T. Kim, and D. N. Basov, Phys. Rev. B **77**, 115121 (2008).
[23]K. Okazaki, S. Sugai, Y. Muraoka, and Z. Hiroi, Phys. Rev. B **73**, 165116 (2006).
[24]C. N. Berglund and H. J. Guggenheim, Phys. Rev. **185**, 1022 (1969).
[25]J. Cao, E. Ertekin, V. Srinivasan, S. Huang, W. Fan, H. Zheng, J. W. L. Yim, D. R. Khanal, D. F. Ogletree, J. C. Grossman, and J. Wu, Nat. Nanotech. **4**, 732 (2009).